Received: 25 January 2022 | Revised: 5 September 2022 | Accepted: 20 October 2022

DOI: 10.1111/pce.14472

ORIGINAL ARTICLE

Plant, Cell & Environment WILEY

Use of thermal imaging and the photochemical reflectance index (PRI) to detect wheat response to elevated CO_2 and drought

Gabriel Mulero[1] | Duo Jiang[1] | David J. Bonfil[2] | David Helman[1,3]

[1]Department of Soil & Water Sciences, Institute of Environmental Sciences, The Robert H. Smith Faculty of Agriculture, Food and Environment, The Hebrew University of Jerusalem, Rehovot, Israel

[2]Department of Vegetable and Field Crop Research, Agricultural Research Organization, Gilat Research Center, Gilat, Israel

[3]The Advanced School for Environmental Studies, The Hebrew University of Jerusalem, Jerusalem, Israel

Correspondence

David Helman, Department of Soil & Water Sciences, Institute of Environmental Sciences, The Robert H. Smith Faculty of Agriculture, Food and Environment, The Hebrew University of Jerusalem, Rehovot, Israel.
Email: David.helman@mail.huji.ac.il

Funding information

Israel Science Foundation, Grant/Award Number: 1792/22

Abstract

The spectral-based photochemical reflectance index (PRI) and leaf surface temperature (T_{leaf}) derived from thermal imaging are two indicative metrics of plant functioning. The relationship of PRI with radiation-use efficiency (RUE) and T_{leaf} with leaf transpiration could be leveraged to monitor crop photosynthesis and water use from space. Yet, it is unclear how such relationships will change under future high carbon dioxide concentrations ($[CO_2]$) and drought. Here we established an $[CO_2]$ enrichment experiment in which three wheat genotypes were grown at ambient (400 ppm) and elevated (550 ppm) $[CO_2]$ and exposed to well-watered and drought conditions in two glasshouse rooms in two replicates. Leaf transpiration (T_r) and latent heat flux (*LE*) were derived to assess evaporative cooling, and RUE was calculated from assimilation and radiation measurements on several dates along the season. Simultaneous hyperspectral and thermal images were taken at ~1.5 m from the plants to derive PRI and the temperature difference between the leaf and its surrounding air ($\Delta T_{leaf-air}$). We found significant PRI and RUE and $\Delta T_{leaf-air}$ and T_r correlations, with no significant differences among the genotypes. A PRI–RUE decoupling was observed under drought at ambient $[CO_2]$ but not at elevated $[CO_2]$, likely due to changes in photorespiration. For a *LE* range of 350 W m^{-2}, the $\Delta T_{leaf-air}$ range was ~10°C at ambient $[CO_2]$ and only ~4°C at elevated $[CO_2]$. Thicker leaves in plants grown at elevated $[CO_2]$ suggest higher leaf water content and consequently more efficient thermoregulation at high $[CO_2]$ conditions. In general, T_{leaf} was maintained closer to the ambient temperature at elevated $[CO_2]$, even under drought. PRI, RUE, $\Delta T_{leaf-air}$, and T_r decreased linearly with canopy depth, displaying a single PRI-RUE and $\Delta T_{leaf-air}$ T_r model through the canopy layers. Our study shows the utility of these sensing metrics in detecting wheat responses to future environmental changes.

KEYWORDS

climate impact, leaf temperature, radiation-use efficiency (RUE), remote sensing

1 | INTRODUCTION

Rising atmospheric carbon dioxide concentrations ($[CO_2]$) and future climatic conditions may interact in complex ways to impact crop production and quality (Ainsworth & Long, 2020; Eller et al., 2020; Tausz-Posch et al., 2020). Forecasting these future impacts requires (1) understanding plant response to biotic and abiotic factors and (2) integrating these understandings into models to represent such impacts. The first is achieved through analysing observational data acquired from natural and manipulative experiments (Kimball, 2016; Uprety et al., 2006). The second is achieved by formulating mathematical equations that describe crop responses to interactive effects (Asseng et al., 2014).

In that sense, remote sensing is a powerful tool that can expand the scope of the observations in time (through continuous monitoring) and space (to a broader scale) and serve as an additional calibration and validation tool. Moreover, since a fundamental challenge for crop modelling is the upscaling of photosynthetic parameters from the leaf to the canopy due to the often non-linear responses among different scales (Jarvis, 1995), the use of remote sensing can aid in filling this scale gap (Thenkabail et al., 2016). Remote sensing can be used to parameterize important traits and processes by relating spectral or thermal metrics derived from sensors onboard flying vehicles to small-scale in situ measurements (Cohen et al., 2015; Gamon et al., 2019; Herrmann & Berger, 2021; Manfreda et al., 2018).

One important photosynthetic parameter for modelling crop production is radiation-use efficiency (RUE). RUE is directly related to plant growth through the assimilation rate relative to the available amount of photosynthetic radiation. As such, RUE is one of the most important physiological traits in the plant's response to climate and environmental change. The use of RUE was proposed by Monteith (1977) as a biophysical metric for modelling gross primary productivity by considering the efficiency of the plant in converting the absorbed intercepted energy (absorbed photosynthetic active radiation [APAR]) into carbon gain (plant biomass):

$$\mathrm{GPP} = \mathrm{APAR} \times \mathrm{RUE}. \quad (1)$$

RUE was shown to vary among species and throughout the season, being highly affected by meteorological and environmental conditions (e.g., water availability, temperature, vapour pressure deficit, and soil mineral content), which makes its modelling a challenging task (Balzarolo et al., 2019; Helman et al., 2017). Crop models use RUE and transpiration efficiency (*TE*) parameters to simulate plant growth and development under different environmental and climate conditions (e.g., Miller et al., 2019). For example, to account for $[CO_2]$ effects, RUE and *TE* are adjusted through linear or near-linear functions (O'Leary et al., 2015). Several studies, however, have shown a complex genotype-by-environment interaction under elevated $[CO_2]$ (eCO_2) and different meteorological conditions that challenge the notion of a simple adjustment of these parameters through a linear function of $[CO_2]$ (Eller et al., 2020; Jiang et al., 2022). Thus, a more robust model representation of such important parameters is required to account for observed climate and $[CO_2]$ effects on crops. The first step would be to monitor RUE and *TE* under different conditions through time and at different scales.

The photochemical reflectance index (PRI), which was first derived and named by Gamon et al. (1992) and Peñuelas et al. (1995), has been shown to be a good proxy for RUE in many studies (Filella et al., 2004; Gamon et al., 1997; Garbulsky et al., 2011). PRI and RUE correlations were found at various levels (Gamon et al., 2005; Kováč et al., 2018; Sukhov et al., 2021) and timescales (Gamon et al., 1992; Magney et al., 2016; Porcar-Castell et al., 2012). Since PRI can be derived from remote sensing, its use opens up a great opportunity for modelling RUE from space (Hilker et al., 2009). The biophysical link between the two is based on the fact that the inhibition mechanism by which plants avoid damage from excess energy is related to pigment changes that affect the absorbance of light at the 530 nm wavelength (Gamon et al., 1992; Peñuelas et al., 1995). More specifically, when plants are exposed to excess light, they apply a photoprotective mechanism by which xanthophyll nonphotochemical quenching occurs (Evain et al., 2004; Kohzuma et al., 2021). The xanthophyll cycle is a photosynthetic process linked to excess light energy—that is, light absorption that is beyond ATP utilization. The mechanism involves the dissipation of excess energy as heat through the de-epoxidation of violaxanthin (xanthophyll pigment) to zeaxanthin. Such a pigment change is reflected in the absorbance of light at the yellow band of the visible spectrum (~531 nm) and is the basis for deriving PRI (Gamon et al., 1992; Peñuelas et al., 1995):

$$PRI = \frac{R_{531} - R_{570}}{R_{531} + R_{570}}, \quad (2)$$

where R_{531} and R_{570} represent the reflectance at the 531 and 570 nm wavelength, respectively.

Although PRI has been proven as a reliable proxy of RUE, as well as of other ecophysiological variables related to photosynthetic activity (Demmig-Adams & Adams, 2006; Kohzuma et al., 2021; Zhang et al., 2017), its performance at the canopy scale is limited by several factors (Hmimina et al., 2014; Magney et al., 2016; Peñuelas et al., 2011; Zhang et al., 2017). Viewing geometry, illumination angle and canopy structure, including leaf shape and orientation, all affect PRI and its ability to accurately track RUE (Amthor, 1994; Garbulsky et al., 2011; Magney et al., 2016; Peñuelas et al., 2011; Zhang et al., 2016). Light interception/absorption across the canopy vertical profile changes at different light conditions, leading to RUE acclimation to prevailing conditions. That may also affect the PRI–RUE relationship. In addition, abiotic stresses were observed to affect the PRI–RUE relationship, challenging the use of PRI in monitoring RUE from space under extreme drought or heatwave conditions (Fréchette et al., 2015; Porcar-Castell et al., 2012).

Evaporative cooling is another important parameter in many models. It occurs through leaf transpiration (T_r), the process by which plants lose water via the stomata opening, a process that releases energy. Such energy release results in the cooling of the leaf surface

(Gates, 1968; Jones et al., 2009; Still et al., 2019). Thus, changes in leaf temperature (or, more precisely, changes in the temperature difference between the leaf and its surrounding environment—$\Delta T_{leaf-air}$) are indicative of evaporative cooling, and different leaf temperature responses to water stress levels may reflect different water-use strategies (Inoue, 1991; Kim et al., 2018; Lapidot et al., 2019; Lima et al., 2016; Sagan et al., 2019). Depending on the level of stress, soil water scarcity (i.e., drought) will make the stomata close as a strategy to conserve water, thereby reducing transpiration and leading to an increase in the leaf temperature (Cornic, 2000; Klein et al., 2011; Matese et al., 2018; Muller et al., 2021b).

Thermocouples equipped with an infrared gas analyser or thermistors can measure such a change. However, this direct-contact estimation is confined to the contact point and does not necessarily represent the entire plant (Kim et al., 2018; Klein et al., 2013). In that sense, thermal imaging can provide a broader view of the thermal response of plants to biotic and abiotic factors at different scales (Lapidot et al., 2019; Lima et al., 2016; Möller et al., 2007; Smigaj et al., 2017; Still et al., 2019; Vialet-Chabrand & Lawson, 2019). Since many studies suggest that future elevated [CO_2] combined with projected climate changes are likely to affect photosynthesis parameters (e.g., RUE) and the water use of plants (affecting the evaporative cooling of the leaves), it is essential to assess how such changes will influence our ability to monitor RUE and evaporative cooling via remote sensing metrics like PRI and $\Delta T_{leaf-air}$.

We conducted two glasshouse experiments in which three wheat cultivars were exposed to a level of [CO_2] expected toward the middle of this century. Plants were subjected to drought (deficit-watered) and compared with plants grown under ambient [CO_2] and well-watered conditions. We measured gas exchange parameters and calculated RUE and evaporative cooling (i.e., latent heat [*LE*]) for the leaves exposed to ambient and elevated [CO_2] under drought and well-watered conditions through time and at different depths within the vertical profile of the canopy. Thermal and spectral images were taken to derive PRI and leaf surface temperature. We compared the cultivars and treatments to answer the following questions:

(1) How does elevated [CO_2] affect the PRI–RUE relationship in wheat leaves grown under well-watered and drought conditions? (2) How does the PRI–RUE relationship change throughout the vertical canopy profile of wheat, and whether the relationship is influenced by [CO_2] and water conditions? (3) How does elevated [CO_2] affect the ability to track changes in evaporative cooling via $\Delta T_{leaf-air}$ in wheat? (4) How does the evaporative cooling–$\Delta T_{leaf-air}$ relationship change within the wheat's canopy profile, and to what extent elevated [CO_2] affect such a relationship?

2 | DATA AND METHODS

2.1 | Experimental setting

Two fully randomized spring wheat [CO_2] enrichment experiments were conducted from March to June of 2021 (Experiment #1) and from February to April 2022 (Experiment #2) in the Faculty of Agriculture, Food and Environment in Rehovot, Israel. Three genotypes bred under the Eastern Mediterranean conditions of Israel, cv. Zahir—an early maturing genotype, cv. Gedera—an intermediate-maturing genotype and cv. Ruta—a late-maturing genotype, were tested in Experiment #1 and two in Experiment #2 (cv. Gedera, as an intermediate-maturing genotype, was excluded since it did not show a significant difference from the other two genotypes in Experiment #1). The genotypes used are commercially available in Israel (Shiff et al., 2021) and have different phenology, productivity and stress tolerances (Aidoo et al., 2017; Bonfil, 2017; Chaudhary et al., 2021; Helman, Bonfil, et al., 2019; Helman, Lensky, et al., 2019). In all experiments, three plants were grown in 4 L plastic pots filled with a peat-based potting mix of a soluble complex of N–P–K fertilizer (14–14–14).

Two glasshouse twin rooms were used, one as control with ambient [CO_2] (aCO_2, 389 ± 27 μmol mol^{-1}) and the other enriched with ~150 μmol mol^{-1} [CO_2] (eCO_2, 554 ± 40 μmol mol^{-1}). We flipped the rooms between Experiments #1 and #2 to have an independent replication of the experiment (Rogers et al., 2021), with a fully randomized factorial design in both replicates. Temperature and relative humidity (RH) were maintained fixed at 26°C/19°C and 60%/80% day/night, respectively, in both rooms for the entire experiment. Sunlight conditions in both rooms were even. No artificial light was used. In each room, two water treatments were applied: (1) well watered to 100% pot holding capacity and (2) drought (i.e., plants were watered to 40% pot holding capacity). Irrigation was applied four times a day through an automatically controlled drip irrigation system.

A summary of the different setups, the number of sampling dates and the sample size for each experiment and type of analysis are presented in Supporting Information: Table S1. Below is a detailed description of the sampling procedure.

2.2 | Multilayer and leaf sampling

Since our goal was to detect changes in RUE and evaporative cooling of wheat exposed to eCO_2 under two water regimes (well-watered and drought), we required our measurements to be representative of the entire plant. The flag leaf (FL), the upper leaf (closest to the head), is usually taken as the representative leaf of the whole plant. However, lower leaves within the canopy profile may respond differently to eCO_2 and water conditions because of their different exposure to light. Ignoring these leaves in models, for example, might result in over/underestimation of the photosynthetic capacity of the whole plant and its true response to changing environmental and climate conditions.

To account for the vertical profile, we divided the plant into vertical layers in which each layer corresponds to a single node on the plant's stem. Thus, for example, the first layer (FL) would correspond to the upper, fully exposed flag leaf, the next layer (L1) to the lower leaf, and so on (Figure 1). Usually, wheat has at least four nodes, meaning four layers. However, since the bottom layer dries out at a very early stage,

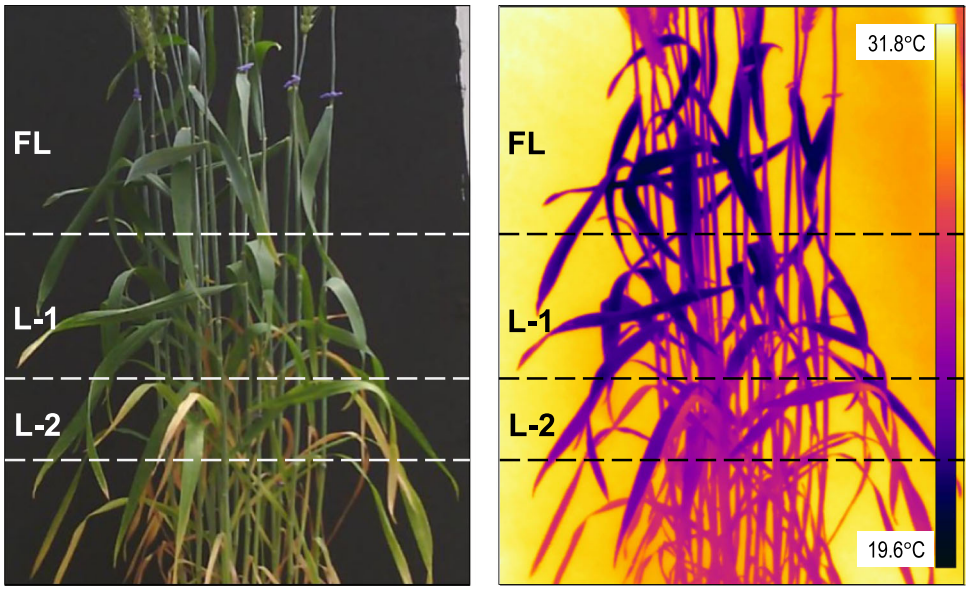

FIGURE 1 RGB (left) and thermal (right) images of a single pot with three wheat plants. The thermal image, taken 67 days from the sowing in Experiment #1, shows a clear temperature difference between the three vertical layers from flag leaf (FL) through layer 1 (L1) and layer 2 (L2). Each vertical layer is distinguished by a nod. Lower layers (L3 and L4) were excluded from the analysis because they dry out early in the season. RGB, red, green, blue.

it is impossible to measure gas exchange in these leaves during the season. We, thus, did not account for the fourth (and below) layer in our analysis but only for FL and L1–L2. In each of these layers, we measured gas-exchange parameters from selected leaves (Section 2.3) and collected hyperspectral and thermal images of the leaves (Sections 2.4 and 2.5) on two dates (days after sowing [DAS] 56 and 72 and DAS 64 and 69 for Experiments #1 and #2, respectively).

Leaf thickness (mm) was measured on DAS 69 (Experiment #2) between two irrigation events (7 AM and 2 PM) on four intact leaves per cultivar from the FL by sampling the mid and top regions from the leaf apex. Measurements were made using a handheld micrometer (Mitutoyo Digital Micrometer Model 293-230-30) with a digital display and a clutch that ensured uniform pressure on the leaves.

2.3 | Gas-exchange measurements

Gas-exchange parameters that included net assimilation (A_n, μmol $m^{-2}\,s^{-1}$) and transpiration (T_r, mmol $m^{-2}\,s^{-1}$) rates were measured around midday (10 AM–2 PM) on randomly healthy and fully expanded upper open/flag leaves on five dates in Experiment #1 (51, 55, 62, 67 and 74 DAS) and Experiment #2 (53, 58, 64, 69 and 74 DAS), from heading to the hard dough. Parameters were measured with an infrared gas analyser (LI-6800; LI-COR) while controlling for the RH inside the chamber to a fixed level of 60% and a flow rate of 500 μmol s^{-1} with CO_2 levels of 400 and 600 μmol mol^{-1} for measurements in the ambient and elevated room, respectively. The temperature inside the chamber was left uncontrolled to assess the evaporative cooling response to eCO_2 under well-watered and drought conditions. We calculated the leaf RUE as the ratio of A_n to PAR and converted it into grams of carbon per megajoule (g C MJ^{-1}). We present evaporative cooling as the energy consumed by *LE* in W m^{-2} (see Section 2.7).

2.4 | Spectral data collection and processing

We used a portable handheld hyperspectral camera, SpecimIQ (Specim Ltd.), to acquire hyperspectral images of the plants. Each image was acquired simultaneously with gas-exchange measurements for [CO_2] × water × genotype treatment, apart from the multilayer images.

The SpecimIQ camera is a handheld push broom system (i.e., along-track scanner) with an integrated operating system and controls that enable easy preprocessing and classification within the camera's software (Behmann et al., 2018; Helman et al., 2022). It covers the wavelengths within the visible–near-infrared range (400–1000 nm), having a total of 204 spectral bands with a 7-nm full-width half-maximum bandwidth and a field of view of 0.55 by 0.55 m at 1 m and a spatial resolution of 512 × 512 pixels. A 10 × 10 cm^2 white reference calibration panel (90% reflectance) was used in the frame to enable transforming irradiance values into relative reflectance. The hyperspectral SpecimIQ camera comes with preinstalled software that allows hyperspectral data capturing and data processing by changing the irradiance values into relative reflectance and other analytical options (Behmann et al., 2018).

Images were taken with the camera fixed on a tripod at a distance of ~1.5 m from the plant to allow a good field of view that will cover the entire extent of the plant. To properly represent illumination conditions, the white reference panel was located next to the sample, and the images were taken using the simultaneous white reference setting of the camera.

The integration time was set between 2 and 10 ms, depending on illumination conditions. Since the Specim IQ software does not support the direct calculation of vegetation indices, reflectance data from the captured images were extracted using the Headwall's Hyperspec III software (Headwall Photonics) by selecting ~30 pixels from the measured leaves as a region of interest (ROI). The PRI was calculated from the spectral data (Section 2.6) per pixel and then averaged over the ROI for each measured leaf.

2.5 | Thermal imaging

We used the same setup as the hyperspectral imaging to acquire thermal images of the plants using a portable FLIR T560 camera (FLIR Systems, Inc.) that has a 640 × 480-pixel resolution and an UltraMax resolution of 1.2 MP, a focal length of 17 mm, 24° × 18° field of view and 30 Hz image frequency. The camera uses an uncooled microbolometer to detect longwave radiation between 7.5 and 14.0 μm with an accuracy of ±2°C or 2% of temperature reading and temperature sensitivity of <0.03°C. It also has a 5 MP digital camera with a built-in light-emitting diode photo/video lamp (technical data taken from the manufacturer). Thermal images were processed using FLIR Tools software (FLIR Systems, Inc.). The manufacturer's default factory setting for correcting outdoor atmospheric effects was maintained. These corrections are often most appropriate for indoor and laboratory environments where the emissivity and environmental conditions are well controlled (Kim et al., 2018). The emissivity was set to a value of 0.95 for leaves, according to Fuchs and Tanner (1966). A specific leaf ROI of 16–30 pixels was selected for each image, depending on the leaf width. The ROI pixels were extracted and exported as a comma-separated value file (for onward analysis), with each cell containing one temperature value per pixel. In the case of the multilayer thermal images, we had a calibration problem in DAS 64 of Experiment #2; thus, we excluded this date from the thermal analysis.

2.6 | PRI

The PRI was developed based on pigment changes due to the epoxidation state of the xanthophyll cycle, which is manifested mainly through changes in the reflectance at the yellow band (Evain et al., 2004; Peñuelas et al., 1995). Since such a process does not affect the absorbance at the end edge of the green spectrum (e.g., at 570 nm; Gamon et al., 1997), a normalized index using these two bands was derived (Peñuelas et al., 1995) (see Equation 2).

2.7 | Evaporative cooling, $\Delta T_{leaf-air}$ and leaf energy balance

We used the thermal images to calculate the average leaf temperature (T_{leaf}) and the difference between T_{leaf} and the air temperature ($\Delta T_{leaf-air}$) as a proxy of evaporative cooling (i.e., *LE*). Since air temperature was maintained unchanged during the day in both rooms (26°C), $\Delta T_{leaf-air}$ is a direct factor of T_{leaf}; yet, we present our results as a function of $\Delta T_{leaf-air}$ because it indicates the relative deviation from the ambient temperature conditions.

$\Delta T_{leaf-air}$ and *LE* are linked through the energy balance as follows:

$$E_{leaf} = H_{leaf} + LE_{leaf} + M_{leaf}, \quad (3)$$

where E_{leaf} is the total available energy for the leaf, which is the sum of the net radiation reaching the leaf's surface. H_{leaf}, LE_{leaf} and M_{leaf} are the sensible, latent and metabolic heat fluxes. Since the heat flux released during the leaf metabolism is very small, M_{leaf} can be neglected. The sensible heat flux, H_{leaf}, is responsible for the change in the ambient air temperature

$$H_{leaf} = \frac{\Delta T_{leaf-air}}{r_a}, \quad (4)$$

where r_a is the leaf's aerodynamic resistance, limiting the heat transfer (i.e., heat dissipation) from the leaf surface to the air. r_a may be a function of many environmental parameters, including wind speed and radiation (Muller et al., 2021a). Still, under fixed environmental conditions without wind, it is mainly a function of leaf characteristics (e.g., leaf structure, geometry, composition, etc.). Combining and rearranging Equations (3) and (4) and neglecting M_{leaf} results in $\Delta T_{leaf-air}$ being a linear function of LE_{leaf}:

$$\Delta T_{leaf-air} = -r_a LE_{leaf} + r_a E_{leaf}. \quad (5)$$

Notice that in Equation (5), for fixed environmental conditions (like in our experiments) and leaves with similar properties (assuming that the leaves grown under eCO_2 are similar to those grown under aCO_2 in terms of structure and composition), the term r_a E_{leaf} is constant. At the same time, $\Delta T_{leaf-air}$ is negatively related through a linear function to *LE*—that is, evaporative cooling—LE_{leaf}.

2.8 | Statistical analysis

All data analyses were performed using the JMP 15 Pro statistical software (SAS Institute). Bar plots of temporal changes in PRI, RUE, T_r and $\Delta T_{leaf-air}$ were computed as a mean of all genotypes together by water and [CO_2] treatment. Tukey's honestly significant difference posthoc test was used in testing for significant differences among groups, and Student's *t*-test was performed for all pairwise comparisons. Tukey's test results are displayed in the bar plot and box plot figures. Analysis of variance was used to assess the effect of [CO_2], water, genotype and their interaction on PRI, RUE, T_r and $\Delta T_{leaf-air}$. A simple linear regression model and the coefficient of determination (R^2) were used to study the relationship between PRI and RUE, and $\Delta T_{leaf-air}$ and T_r or *LE* at probability levels of $^*p < 0.1$, $^{**}p < 0.05$ and $^{***}p < 0.001$. Following the small size of the multilayer samples, a more relaxed probability level of $p < 0.1$ was used in its analysis. Analysis of covariance was used to test for significant differences between the slopes of two linear fits.

3 | RESULTS

3.1 | How does elevated [CO_2] affect PRI and RUE under well-watered and drought conditions?

FL PRI and RUE varied throughout the plant's growth and development, while a decreasing trend was evident for both PRI and RUE, particularly under eCO_2 (Figure 2). Both [CO_2] and drought significantly affected RUE (Table 1), with eCO_2 increasing and drought reducing the RUE, respectively. No significant effect of [CO_2] or water was found on PRI. Multifactor interactions were all nonsignificant for PRI and RUE (Table 1).

PRI and RUE were linearly correlated through a positive relationship (Figure 3a). This was significant, however, only under eCO_2 ($R^2 = 0.38$; $p < 0.001$). When separating the data per water treatment, the PRI–RUE relationship was also significant at aCO_2 under well-watered conditions ($R^2 = 0.32$, $p < 0.05$; Figure 3b), while at eCO_2, the relationship remained significant under both water treatments (Figure 3c).

The R^2 of the linear regressions per genotype ranged from 0.23 to 0.88 for well-watered and both [CO_2] treatments but was primarily insignificant for the drought treatment under aCO_2 (Supporting Information: Figure S1). At eCO_2, the per-water-treatment models were all significant and similar ($p > 0.1$ for the difference among the slopes), except for cv. Ruta, such that a single per-cultivar model can describe RUE as a function of PRI under both water conditions.

3.2 | How does the PRI–RUE relationship change throughout the vertical canopy profile?

RUE and PRI seemed to decrease within the vertical canopy profile from FL to L2 (Supporting Information: Figure S2). The multilayer data showed positive PRI–RUE linear regression models for almost all layers (Figure 4a–d). A gradual decrease through the layers from FL to L2 suggests that both parameters decrease linearly throughout the vertical profile. However, such a linear correlation was significant for all layers at aCO_2 and only for FL and L1 at eCO_2 under well-watered conditions and was significant only for FL at eCO_2 under drought conditions (Figure 4e).

3.3 | How does elevated [CO_2] affect evaporative cooling and $\Delta T_{leaf-air}$ relationships?

T_r and $\Delta T_{leaf-air}$ varied largely throughout the season, with a greater irregularity observed in $\Delta T_{leaf-air}$ (Figure 5). [CO_2] × water and [CO_2] × genotype interactions were significant for $\Delta T_{leaf-air}$ and water × genotype for T_r (Table 1), where $\Delta T_{leaf-air}$ was less negative at eCO_2 under well-watered conditions, but not so much under drought. In both cases, however, the difference in $\Delta T_{leaf-air}$ among the CO_2 treatments was mostly statistically insignificant (Figure 5a,b). $\Delta T_{leaf-air}$ and T_r were significantly correlated through a negative linear relationship in almost all dates, regardless of the [CO_2] level (except for 67 DAS under eCO_2), though the relationships differed among dates and treatments (Figure 6), and were less clear in Experiment #2 (Supporting Information: Figure S3). Including all dates together generated a linear fit of $R^2 = 0.32$ ($p < 0.001$; Supporting Information: Figure S4).

A narrower range in $\Delta T_{leaf-air}$ was observed per genotype at eCO_2, especially under drought. Surprisingly, the mean $\Delta T_{leaf-air}$ was 1.5–2.0°C higher at aCO_2 than at eCO_2 in the drought treatment and was generally the same under well-watered conditions (Supporting Information: Figure S5). The only exception was the early maturing genotype of Zahir, which showed a higher mean $\Delta T_{leaf-air}$ of ~1.2°C at aCO_2 compared to eCO_2 even under well-watered conditions (Supporting Information: Figure S5b).

3.4 | How does the evaporative cooling–$\Delta T_{leaf-air}$ relationship change within the canopy profile?

Differences in T_{leaf} throughout the vertical canopy profile were evident in the thermal images (Figure 1), with cooler leaves at the top and warmer leaves at the bottom of the canopy (Supporting Information: Figure S6). T_r generally decreased while $\Delta T_{leaf-air}$ increased from top to bottom (FL to L2), with $\Delta T_{leaf-air}$ increase being more clear under well-watered conditions (Supporting Information: Figure S6b).

As with the PRI–RUE, a single linear model describes the $\Delta T_{leaf-air}$–*LE* relationship throughout the layers (black lines in Figure 7). However, $\Delta T_{leaf-air}$ was much more responsive to evaporative cooling (calculated as *LE*) under aCO_2 than under eCO_2 (steeper slope of the black line in Figure 7a compared to the slope of the black line in Figure 7b). For a change in evaporative cooling (*LE*) of ~350 W m^{-2}, the range in the $\Delta T_{leaf-air}$ response was around 10°C at aCO_2, while it was only ~4°C under eCO_2. Leaf thickness measurements showed a significant effect of [CO_2], with thicker leaves found under eCO_2 (Table 2), which suggests an increase in the leaf water content under eCO_2, especially under well-water conditions (a significant [CO_2] × water interaction; Table 2).

4 | DISCUSSION

4.1 | PRI–RUE relationship in wheat is preserved under drought due to the high [CO_2]

Previous studies have shown close relationships between PRI and photosynthetic activity, including relationships with net assimilation, chlorophyll content and RUE from the leaf to the canopy and the ecosystem scale (Gamon et al., 1997; Garrity et al., 2011; Wu et al., 2015; Zhang et al., 2017). Our study concurs with these previous results. Significant leaf-level PRI–RUE correlations were observed in three wheat genotypes bred under semiarid Mediterranean conditions with differing phenological characteristics and stress

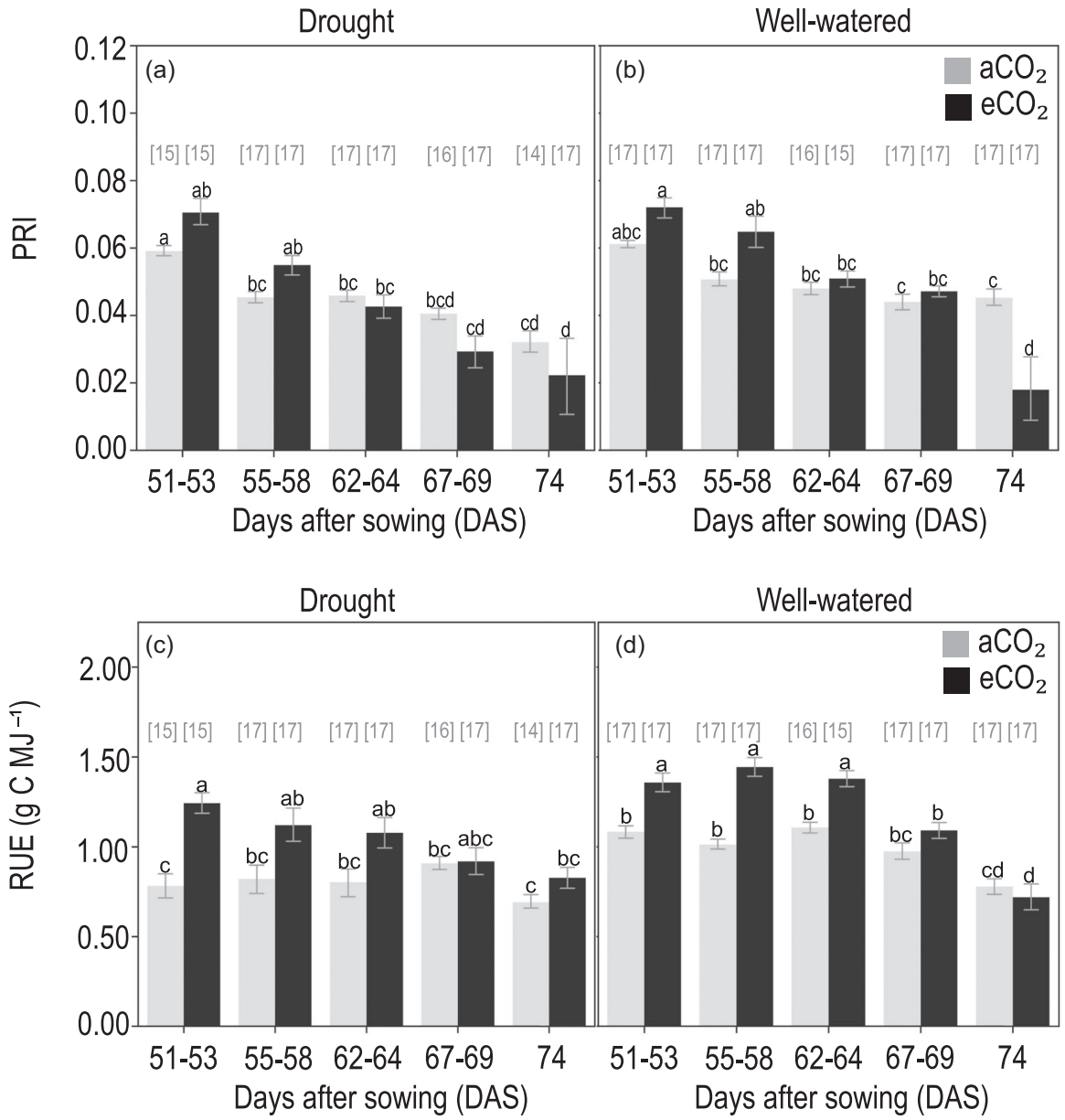

FIGURE 2 PRI (a, b) and RUE (g C MJ^{-1}) (c, d) of wheat plants exposed to elevated (black) and ambient (grey) [CO_2] levels across five dates in Experiment #1 (51, 55, 62, 67 and 74 DAS) and Experiment #2 (53, 58, 64, 69, 74 DAS). Plants were subjected to drought (a, c) and well-watered (b, d) conditions. The numbers in the brackets represent the sample size (*N*). Error bars represent the standard error over all the measurements from both experiments. Different letters indicate significant differences at $p < 0.05$ from Tukey's HSD test per treatment. DAS, days after sowing; HSD, honestly significant difference; PRI, photochemical reflectance index; RUE, radiation-use efficiency.

tolerances (Figures 3 and 4). However, this is the first time such a relationship has been reported for plants grown under elevated [CO_2]. Interestingly, the PRI–RUE relationships were similar at ambient and elevated [CO_2], with the only exception being the plants grown under consistent drought that showed a decoupling in the ties of PRI and RUE (Figure 3b,c).

A decoupling in PRI–RUE under drought conditions was previously reported in trees (Fréchette et al., 2015; Porcar-Castell et al., 2012). As far as we know, such a decoupling was never reported in field crops or, more specifically, in wheat. The interesting part of these results is that such a decoupling was absent in plants grown under elevated [CO_2]. Water deficit, extreme temperature and intense light may cause the decoupling of photosynthetic electron transport and ribulose 1,5-bisphosphate carboxylase/oxygenase (RuBisCO) carboxylation. Such decoupling is most likely to result in anomalies in the PRI–RUE relationship (Huang et al., 2019; Kováč et al., 2018). Under stress conditions (e.g., drought), alternative electron pathways of heat dissipation come into play (Fréchette et al., 2015).

For example, an important mechanism not detected by PRI involves the increase in electron transport around photosystem I, which may be a significant energy sink when plants are exposed to

TABLE 1 Statistics *F* ratio and *p* value > *F* ratio of full factorial three-way ANOVA for RUE (g C MJ^{-1}; *N* = 325) PRI (unitless; *N* = 325), $\Delta T_{leaf-air}$ (°C; *N* = 325) and T_r (mmol m^{-2} s^{-1}; *N* = 325)

	RUE		PRI		$\Delta T_{leaf-air}$		T_r	
Effect	***F***	***p* > *F***	***F***	***p* > *F***	***F***	***p* > *F***	***F***	***p* > *F***
$[CO_2]$	38.2	**<0.001**	0.1	0.73	0.1	0.74	7.7	**<0.01**
Water (W)	26.6	**<0.001**	3.0	0.09	103.6	**<0.001**	137.8	**<0.001**
Genotype (G)	11.6	**<0.001**	2.4	0.09	3.2	**0.04**	6.9	**<0.01**
$[CO_2]$ × W	0.5	0.48	0.01	0.93	7.4	**<0.01**	1.2	0.28
$[CO_2]$ × G	0.7	0.48	1.8	0.16	5.5	**<0.01**	1.0	0.36
W × G	0.3	0.74	1.8	0.17	1.0	0.39	6.3	**<0.01**
$[CO_2]$ × W × G	1.1	0.35	1.1	0.35	2.6	0.08	1.9	0.15

Note: Statistically significant effects at $p > 0.05$ are marked in bold.

Abbreviations: ANOVA, analysis of variance; PRI, photochemical reflectance index; RUE, radiation-use efficiency; T_{leaf}, average leaf temperature; $\Delta T_{leaf-air}$, the difference between T_{leaf} and the air temperature.

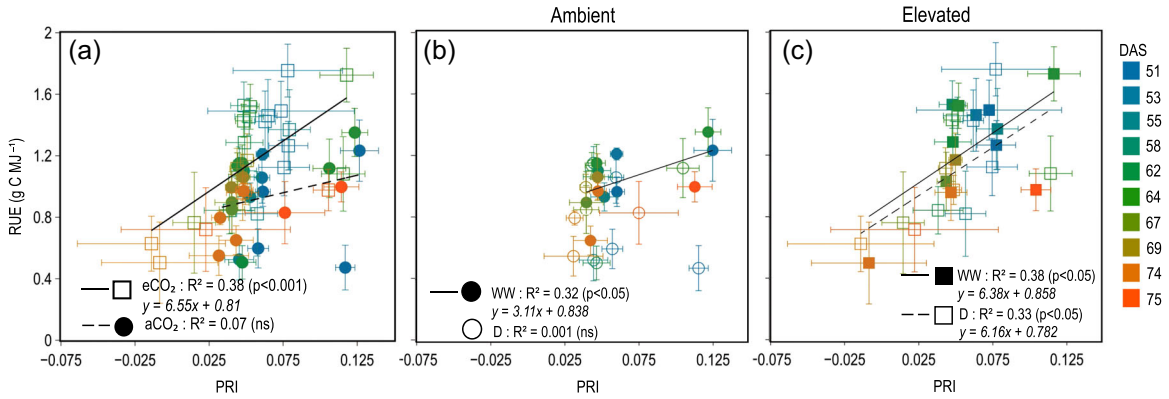

FIGURE 3 Linear regressions of PRI versus RUE for (a) ambient (square) and elevated (circle) $[CO_2]$ treatment for both water treatments together and for (b) ambient and (c) elevated $[CO_2]$ by water treatment (WW: well watered; D: drought). Error bars represent the standard error. The colour of each symbol indicates its specific date as days after sowing (DAS). The R^2 of the correlation, the linear fit equation and its significance level are presented in the plots. PRI, photochemical reflectance index; RUE, radiation-use efficiency. [Color figure can be viewed at wileyonlinelibrary.com]

extreme light, temperature or drought conditions (Fréchette et al., 2015; Takahashi & Badger, 2011). Another such photoprotective mechanism is photorespiration. Photorespiration, once taught to be a wasteful process in which carbon is released from the plant back to the environment (Busch, 2013), is now acknowledged as an essential photoprotective mechanism. It prevents the production and accumulation of reactive oxygen species in the peroxisome when plants are exposed to a stress (Eisenhut et al., 2017; Voss et al., 2013). Since such a process does not involve pigment changes, spectral-based indices such as PRI cannot track it. This might be a serious limitation of remote sensing of critical photosynthetic parameters such as RUE.

However, in our study, the exerted drought did not affect the PRI–RUE relationship when plants were exposed to an elevated $[CO_2]$ of +150 ppm. Such an observation was consistent in all three cultivars in two independent replicates of the same experiment. PRI–RUE correlations, however, were nonsignificant in L1 and L2 under drought even at elevated $[CO_2]$ (Figure 4), suggesting that xanthophyll nonphotochemical quenching was significantly affected with leaf aging. If photorespiration was the primary photoprotective response to drought at ambient $[CO_2]$, this was unlikely the case in FL at elevated $[CO_2]$. Usually, drought leads to stomatal closure, which limits the diffusion of CO_2 to the chloroplast. This results in increased photorespiration due to a reduced stromal C:O concentration ratio (Kangasjarvi et al., 2012), which, in turn, shifts RuBisCo towards preferring oxygenation over carboxylation (Busch, 2020; Von Caemmerer, 2000). However, when intercellular CO_2 concentration is high enough due to an enriched $[CO_2]$ environment, for example, the abovementioned oxygenation to carboxylation shift would be more limited under drought (Dusenge et al., 2019; Liu et al., 2018; Wada et al., 2020). Hence, under high $[CO_2]$ (in our case, 550 µmol mol^{-1}), the PRI–RUE relationship would be maintained even under a severe drought, such as that experienced by the plants in the current experiment (40% of the pot holding capacity). The xanthophyll nonphotochemical quenching becomes the primary inhibition

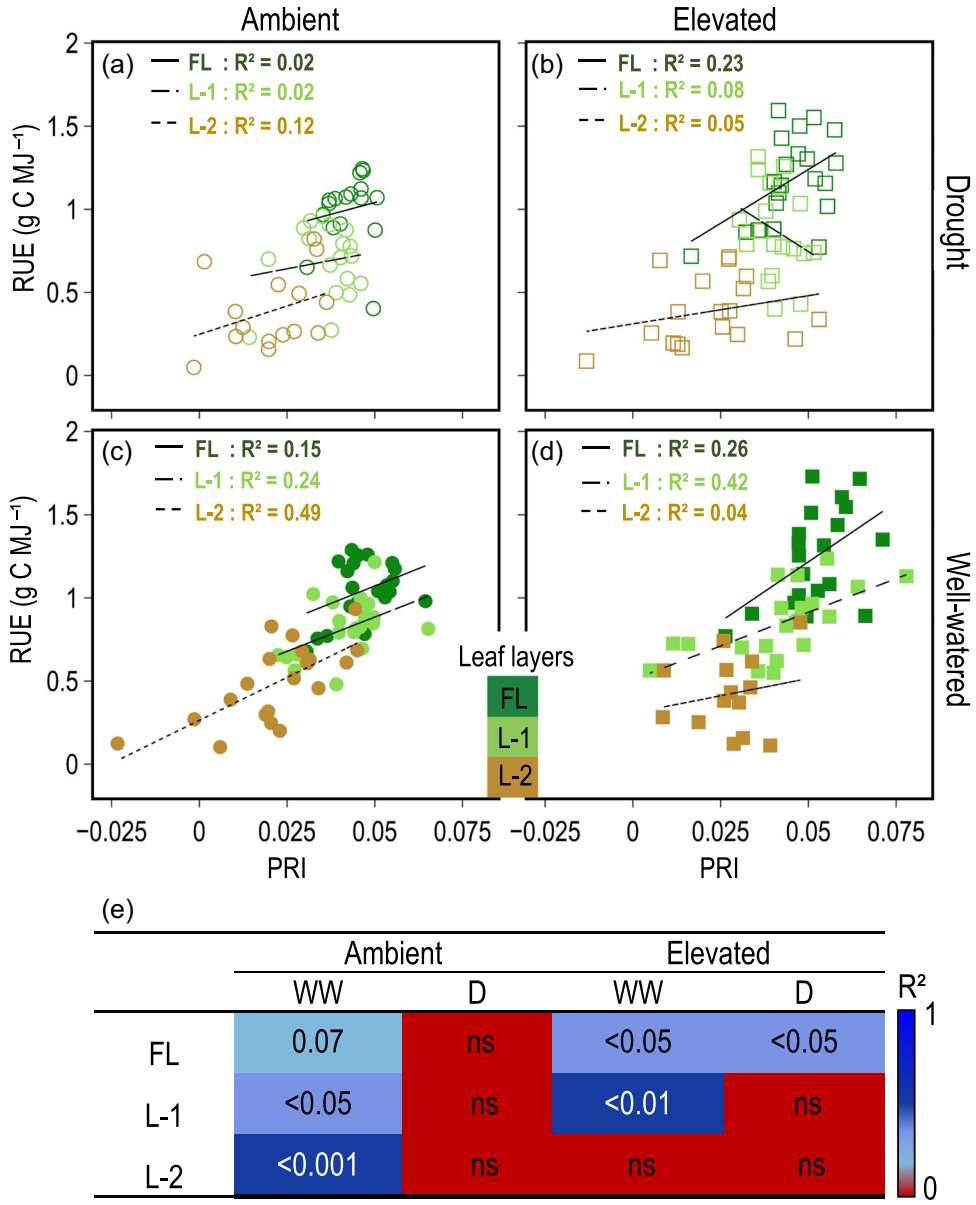

FIGURE 4 Linear regression of PRI versus RUE at the different leaf layers (a–d) from the flag leaf (FL; dark green) to the two bottom layers (L1 in light green and L2 in brown) of plants exposed to elevated (squares) and ambient (circles) [CO_2] under drought (open symbols) and well-watered conditions (closed symbols). (e) Table showing the R^2 of the correlations obtained in (a–d) and the corresponding p values. Nonsignificant correlations ($p > 0.1$) are marked with ns. ns, Not significant; PRI, photochemical reflectance index; RUE, radiation-use efficiency. [Color figure can be viewed at wileyonlinelibrary.com]

mechanism again, while photorespiration is vastly reduced under elevated [CO_2].

Another possible explanation for the unobserved decoupling of PRI and RUE under drought and elevated [CO_2] could be the increase in water retention in the soil and leaves, which would reduce water stress and, consequently, photorespiration. It is well known that plants exposed to elevated [CO_2] transpire less and retain more water in the soil (Blumenthal et al., 2018; Liu et al., 2018; Paudel et al., 2018). An elevated [CO_2] has been shown to increase the TE of plants by closing the stomata (Ainsworth & Rogers, 2007; Leakey et al., 2009), thereby conserving more water in the soil (Christy et al., 2018; Tausz-Posch et al., 2013). The usually increased assimilation and reduced transpiration under elevated [CO_2] has been suggested to improve crop water productivity—the ratio between the yield production and water use (Deryng et al., 2016), thus benefiting crops under drought (Wall et al., 2006). The low leaf temperature responsiveness to water stress under elevated [CO_2] observed in our study (Figure 5a and Supporting Information: Figure S6a) partly supports this explanation. This may indicate higher water availability in the soil for plants grown under elevated [CO_2] and/or higher relative water content in the leaves of these plants (as will be discussed further in the following subsection).

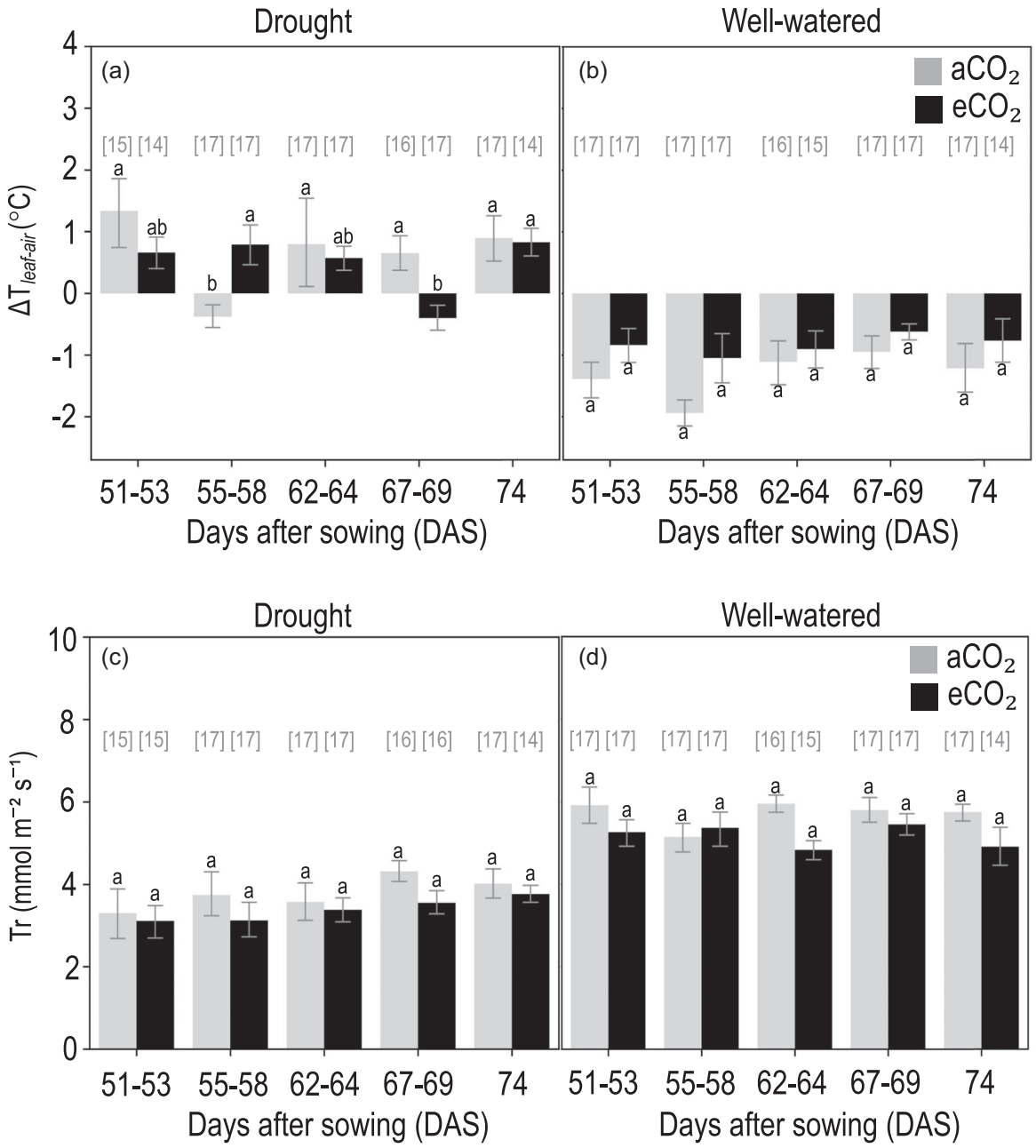

FIGURE 5 $\Delta T_{leaf-air}$ (°C) (a, b) and T_r (mmol m^{-2} s^{-1}) (c, d) of wheat plants exposed to elevated (black) and ambient (grey) [CO_2] levels across five dates in Experiment #1 (51, 55, 62, 67 and 74 DAS) and Experiment #2 (53, 58, 64, 69 and 74 DAS). Plants were subjected to drought (a, c) and well-watered conditions (b, d). The numbers in the brackets represent the sample size (*N*). Error bars represent the standard error over all the measurements from both experiments. Different letters indicate significant differences at $p < 0.05$ from Tukey's HSD test per treatment. DAS, days after sowing; HSD, honestly significant difference; T_r, leaf transpiration; $\Delta T_{leaf-air}$, the difference between T_{leaf} and the air temperature.

The fact that the PRI–RUE relationship is maintained under drought at a high [CO_2] such as expected in the next two to three decades is encouraging for future remote sensing monitoring of crop systems. However, conditions by which the correlation between PRI and RUE decouples in wheat as well as the mechanisms by which an elevated [CO_2] affects such a decoupling still need to be further investigated under both, controlled and field experimental settings. Specifically, we point to measuring photorespiration under different water and [CO_2] conditions to assess or reject our above-mentioned hypotheses.

4.2 | Leaf temperature is less responsive to evaporative cooling under elevated [CO_2]

The relationship between $\Delta T_{leaf-air}$ and T_r was, as expected, negative (Figure 6). Such a negative correlation was regardless of the water condition and was observed at both levels of [CO_2]. Such leaf cooling is a well-known heat dissipation mechanism used by plants (Dusenge et al., 2019; Urban et al., 2017). As such, leaf temperature and $\Delta T_{leaf-air}$ may be used to assess transpiration rate (e.g., Lapidot

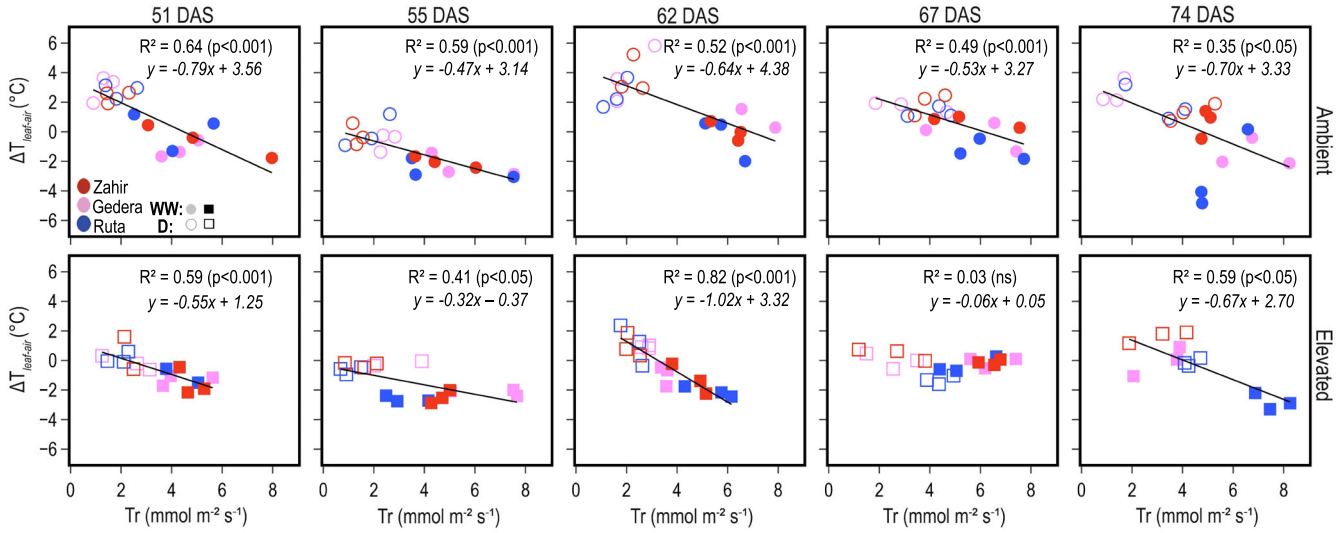

FIGURE 6 Per-date (DAS) linear regressions of leaf $\Delta T_{leaf-air}$ (°C) versus T_r (mmol m^{-2} s^{-1}) for plants exposed to ambient and elevated [CO_2] in Experiment #1. Genotypes are indicated in different colours—Zahir: red; Gedera: purple; Ruta: blue. Only statistically significant regression lines are shown. DAS, days after sowing; $\Delta T_{leaf-air}$, the difference between T_{leaf} and the air temperature. DAS, days after sowing; HSD, honestly significant difference; T_r, leaf transpiration; $\Delta T_{leaf-air}$, the difference between T_{leaf} and the air temperature. [Color figure can be viewed at wileyonlinelibrary.com]

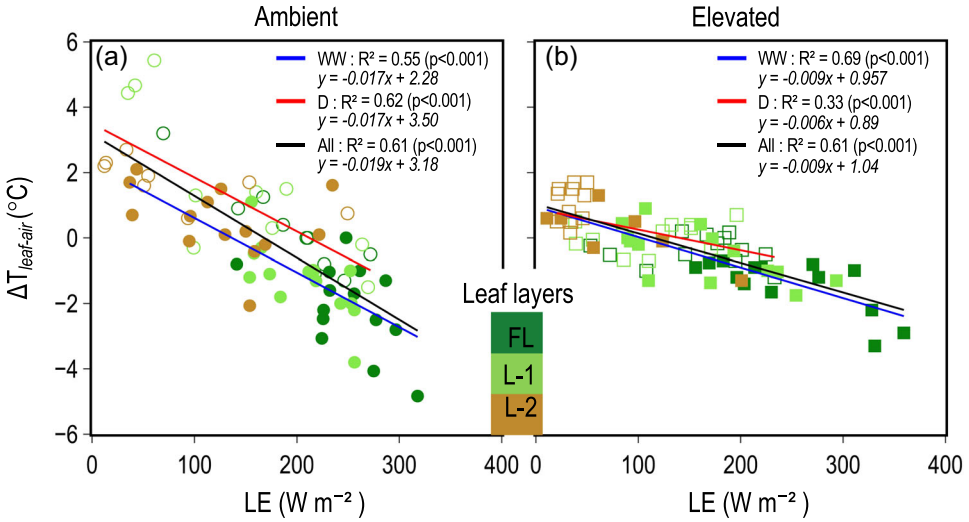

FIGURE 7 $\Delta T_{leaf-air}$ (°C) relationship with evaporative cooling, measured as *LE* (W m^{-2}) of plants exposed to (a) ambient and (b) elevated [CO_2] under drought (open symbols) and well-watered conditions (closed symbols). Layers are distinguished by different colours (FL—dark green; L1—light green; and L2—brown). Notice that for a similar range in *LE* (*x*-axis), plants grown at elevated [CO_2] had a narrower range in $\Delta T_{leaf-air}$ (°C), implying a more efficient thermoregulation response to transpiration changes. LE, latent heat; $\Delta T_{leaf-air}$, the difference between T_{leaf} and the air temperature. [Color figure can be viewed at wileyonlinelibrary.com]

et al., 2019) and other gas-exchange parameters such as stomatal conductance and photosynthesis (Kim et al., 2018). As may be expected, warmer leaf temperatures are usually observed in plants exposed to drought stress (Lapidot et al., 2019) or high [CO_2] levels (Grey et al., 2016). The latter is because plants close their stomata and reduce their transpiration in response to elevated [CO_2] (Jones et al., 1984; Long et al., 2004).

In our case, the leaves of plants grown under drought were warmer (Figure 5a); yet, those grown under elevated [CO_2] were relatively cooler than ambient [CO_2]-grown leaves even under drought. A plausible explanation for the somewhat cooler temperatures of the elevated [CO_2]-grown leaves may be a high water content in these leaves. Since high [CO_2] causes the stomata to close, plants may retain more water in their tissues, including their leaves, thereby regulating their internal temperature more closely to ambient conditions even under drought (Liu et al., 2018; Paudel et al., 2018; Swann et al., 2016).

Though we did not assess leaf water content directly in this study, the thicker leaves found under elevated [CO_2] partly support

TABLE 2 Statistics *F* ratio and *p* value > *F* ratio of full factorial three-way ANOVA for leaf thickness from Experiment #2

Effect	*F*	*p* > *F*
$[CO_2]$	10.95	**0.003**
Water (W)	0.95	0.34
Genotype (G)	1.34	0.26
$[CO_2] \times W$	5.32	**0.03**
$[CO_2] \times G$	0.037	0.85
$W \times G$	0.052	0.82
$[CO_2] \times W \times G$	0.091	0.77

Note: Statistically significant effects at $p > 0.05$ are marked in bold. The sample size is $N = 32$ (two leaves × two pots × two genotypes × two water treatments × two CO_2 treatments).

Abbreviation: ANOVA, analysis of variance.

that (Table 2). In addition, the higher PRI of the leaves grown under elevated $[CO_2]$ than those grown under ambient $[CO_2]$ partly implies that the leaf water content among the $[CO_2]$ treatments differed. Previous studies show that leaves with higher water content also have higher PRI. In fact, a linear relationship was found between the two (Zhang et al., 2018). Further, if we consider that the total available energy (*E*) was the same for all plants since temperature, RH and radiation were all the same in both rooms (i.e., $E = E^{eCO_2} = E^{aCO_2}$), then for a specific evaporative cooling—*LE*, we can rewrite Equation (5) for two leaves, one grown under elevated and another grown under ambient $[CO_2]$, as follows:

$$\Delta T_{leaf-air}{}^{eCO_2} = r_a{}^{eCO_2}(E - LE), \tag{6}$$

$$\Delta T_{leaf-air}{}^{aCO_2} = r_a{}^{aCO_2}(E - LE). \tag{7}$$

We can then combine the two equations and eliminate similar terms:

$$\Delta T_{leaf-air}{}^{aCO_2}/\Delta T_{leaf-air}{}^{eCO_2} = r_a{}^{aCO_2}/r_a{}^{eCO_2}. \tag{8}$$

Notice that Equation (8), which describes the change in $\Delta T_{leaf-air}$ for a similar shift in *LE*, shows that the difference (ratio) in $\Delta T_{leaf-air}$ between the two leaves is a result only of the difference in the aerodynamic resistance among the leaves. This means that something in the leaf grown under elevated $[CO_2]$ was changed. Such a change affected its thermoregulation response by affecting its aerodynamic resistance and, consequently, its temperature response to evaporative cooling. Indeed, a shift in ~350 W m^{-2} in *LE* was found to change $\Delta T_{leaf-air}$ by more than 10°C at ambient $[CO_2]$, while a similar change in *LE* changed $\Delta T_{leaf-air}$ by only ~4°C for plants grown under elevated $[CO_2]$ (Figure 7). In the case where a leaf exposed to elevated $[CO_2]$ had increased its water content compared to a leaf grown at ambient $[CO_2]$, as we suggest here through the thicker leaves observed under elevated $[CO_2]$ (Table 2), this could explain the more efficient thermoregulation of the high $[CO_2]$-grown leaf at different levels of *LE* (i.e., it explains the much narrower $\Delta T_{leaf-air}$ response to *LE* under elevated $[CO_2]$ than under ambient $[CO_2]$).

Indeed, several factors, asides from the water supply, may influence the temperature difference between the leaf and the surrounding environment. These include biotic factors such as the physical location of the plant, its leaf characteristics and canopy structure, as well as abiotic factors, including weather and $[CO_2]$, which may interact with the crop in complex ways (Muller et al., 2021a; Still et al., 2019, 2021). Because plant position and canopy structure, as well as the weather conditions, were nearly the same for plants in both rooms (as much as this can be achieved in a controlled glasshouse experiment), a change in leaf characteristics would be the most reasonable explanation for the different leaf temperature responses to a similar evaporative cooling. Of course, such a claim should be investigated and confirmed directly while further assessed under field conditions. Yet, if true, this is an essential outcome because a future rise in $[CO_2]$ can impact small yet important physiological traits that can lead to significant water and energy balance changes at a much larger scale.

4.3 | Multilayer vertical aspect

The expectation that an ongoing rise in $[CO_2]$ and more frequent and severe drought in many crop areas worldwide will interact with crops in a complex manner has important implications (Eller et al., 2020). This incumbrances interaction at the leaf level and the canopy, and the entire ecosystem scales (Rogers et al., 2017). High $[CO_2]$ may have a contrasting effect on leaf temperature. Typically, a rise in $[CO_2]$ would lead to warmer leaf temperatures due to reduced stomatal conductance and reduced transpiration (evaporative cooling). At the same time, we may expect more water to be retained in the soil due to reduced transpiration (Kimball, 2016; Tausz-Posch et al., 2020). Thus, the additional water in the soil is likely to cool the leaves through surface evaporation even higher under elevated $[CO_2]$, ameliorating the stomata closure's warming effect.

On top of that, a discrepancy may exist among the different scales. For example, a free-air CO_2 enrichment experiment conducted on broadleaf deciduous trees showed that leaf stomatal conductance was reduced by 40% under elevated $[CO_2]$, while canopy-scale conductance was reduced by only 10% (Wullschleger et al., 2002). Such a scale discrepancy means that the microclimate within the canopy cannot be assumed to be equal for all vertical layers. Hence, the leaf-level processes need to be correctly integrated to represent the whole canopy by considering the multilayer vertical aspect (Katul et al., 2012).

Simulating the effects of elevated $[CO_2]$ on crop growth and yield in process-based models involves introducing new factors or multipliers and modifying specific components, one of which is integrating the leaf response into the whole-plant scale (Tubiello & Ewert, 2002). To effectively scale up responses of essential parameters like evaporative cooling, transpiration, and RUE to a simultaneous effect of drought and $[CO_2]$, mechanistic models need

to account for the response of each of those parameters throughout the different vertical layers in the canopy. Only by considering the various processes throughout the different layers can a more realistic view of the whole-canopy response be achieved (Ewert et al., 2002; Katul et al., 2012).

Our results show apparent differences in evaporative cooling, leaf temperatures, PRI and RUE across the canopy vertical layers supporting the abovementioned claim. Further, they contradict the widespread idea that leaves at the top of the canopy (e.g., flag leaves in wheat) represent the whole plant. Such an assumption is essential, for example, in 'big-leaf' and 'two big-leaf' models, which are very popular simulation models used to study crop responses to future conditions (Rogers et al., 2017). Models like the one proposed by Monteith (e.g., Helman et al., 2017; Miller et al., 2019) have been used to scale parameters assuming that the overall canopy term is equivalent to the top leaf layer (i.e., the FL), which represents all other leaves in the canopy. Yet, many studies, including ours, have shown that a single leaf could not be used to accurately represent all leaves in the canopy (Gara et al., 2019; Gitz III et al., 2016).

A common challenge for models in the upscaling of photosynthetic and other leaf gas exchange parameters is the heterogeneity of processes and the non-linear scaling response from the leaf to the canopy (Jarvis, 1995; Niinemets et al., 2015). Accordingly, multilayer models are more accurate because they consider the response at the various layers within the canopy profile (Bonan et al., 2021). The problem is that such an approach is complex, and the retrieval of multilayer parameters is not straightforward. Remote sensing may aid in this task. Yet, the parameterization should be conducted with proper calibration and validation set at the various scales. Here we aimed to add to this effort by looking at leaves from different layers and relating the observed processes to spectral-based and thermal information. The good news is that our results show that evaporative cooling, leaf temperatures, PRI and RUE all decrease linearly with canopy depth, at least in wheat. This means that a simple linear model can be used to account for the response of these parameters to abiotic changes throughout the vertical canopy profile in wheat. Though requiring further assessment in the field, this first attempt to model evaporative cooling and RUE response to $[CO_2]$ and drought throughout the canopy profile of wheat can be used to improve multilayer modelling.

5 | CONCLUDING REMARKS

We found significant PRI–RUE relationships in our experiment as in previous studies. However, this is the first time such relationships are reported for plants exposed to elevated $[CO_2]$ and, more specifically, in wheat. In that context, PRI–RUE relationships in typical Israeli wheat genotypes differed among $[CO_2]$ levels, with a steeper PRI–RUE linear regression model observed in plants exposed to elevated $[CO_2]$, meaning higher sensitivity of PRI to RUE variations. We also found a decoupling between PRI and RUE in wheat plants exposed to drought at ambient $[CO_2]$, a phenomenon previously reported in trees. Such a decoupling did not occur under elevated $[CO_2]$, indicating that the PRI–RUE decoupling under drought may be due to enhanced photorespiration. This means that remote sensing of RUE might be enabled even under stress conditions in a future world of higher $[CO_2]$.

Evaporative cooling was also significantly correlated with leaf surface temperature, which opens up new opportunities for thermal remote sensing to detect crop transpiration response to biotic and abiotic stresses. In that sense, water conditions did not affect the leaf temperature-latent heat flux relationships. However, leaf temperature was much less responsive to evaporative cooling under elevated $[CO_2]$ for unclear reasons. The leaf temperature of plants exposed to elevated $[CO_2]$ was kept very close to the ambient air temperature even for a *LE* change of 350 W m^{-2}. Leaf thickness, energy balance calculations and PRI results suggest that leaves exposed to elevated $[CO_2]$ had higher relative water content, which affected their thermoregulation response to soil water conditions. This suggestion, however, warrants further investigation with more focused measurements to confirm or reject such a hypothesis.

Multilayer measurements resulted in PRI–RUE and leaf temperature–*LE* linear relationships throughout the vertical canopy profile. This means that a simple linear model can describe these parameters throughout the canopy. Further, the gradual decrease in RUE and *LE* with the canopy depth suggests that the response of these parameters is linear throughout the vertical canopy profile. Of course, this may change according to the plant position, sun angle and so on. Yet, the linear relationship with the sensing-based metrics (PRI and thermal leaf image) implies that such means can be easily used to parametrize and upscale important biophysical parameters like transpiration and RUE using remote sensing in the field. Further, the use of new remote sensing tools such as LiDAR may greatly assist in bridging between the scales because it enables assessing the sensing metrics at a three-dimensional level in the field. This may add substantial power to current remote sensing efforts of photosynthesis monitoring.

Finally, the complex whole-plant response alongside the different leaf trait responses across the crop vertical profile raises the need for further research to uncover new underlying mechanisms of crop response to climate conditions under future elevated $[CO_2]$.

ACKNOWLEDGEMENTS

This research is currently supported by the Israel Science Foundation (grant number 1792/22). D. J. was funded by the China Scholarship Council (CSC No. 202008280005). The authors thank Gil Lerner for his support with the irrigation system and Leon Cohen for assisting with the glasshouse room conditions. The authors also thank the editor, Elizabeth Ainsworth, and three anonymous reviewers for their valuable comments and suggestions, which helped improve the quality of this manuscript. G. M. is a Ph.D. student- under the supervision and guidance of D. H.

CONFLICT OF INTEREST

The authors declare no conflict of interest.

DATA AVAILABILITY STATEMENT

The data supporting this study's findings are available from the corresponding author upon reasonable request.

ORCID

Gabriel Mulero http://orcid.org/0000-0002-2935-6233
David Helman http://orcid.org/0000-0003-0571-8161

REFERENCES

Aidoo, M.K., Quansah, L., Galkin, E., Batushansky, A., Wallach, R., Moshelion, M. et al. (2017) A combination of stomata deregulation and a distinctive modulation of amino acid metabolism are associated with enhanced tolerance of wheat varieties to transient drought. *Metabolomics*, 13, 138. Available from: https://doi.org/10.1007/s11306-017-1267-y

Ainsworth, E.A. & Long, S.P. (2020) 30 years of free-air carbon dioxide enrichment (FACE): what have we learned about future crop productivity and its potential for adaptation? *Global Change Biology*, 27(1), 27–49. Available from: https://doi.org/10.1111/gcb.15375

Ainsworth, E.A. & Rogers, A. (2007) The response of photosynthesis and stomatal conductance to rising [CO_2]: mechanisms and environmental interactions: photosynthesis and stomatal conductance responses to rising [CO2]. *Plant, Cell & Environment*, 30, 258–270. Available from: https://doi.org/10.1111/j.1365-3040.2007.01641.x

Amthor, J.S. (1994) Scaling CO_2–photosynthesis relationships from the leaf to the canopy. *Photosynthesis Research*, 39, 321–350. Available from: https://doi.org/10.1007/BF00014590

Asseng, S., Zhu, Y., Basso, B., Wilson, T. & Cammarano, D. (2014) Encyclopedia of agriculture and food systems. In: Van Alfen, N.K. (Ed.) *Simulation modeling: applications in cropping systems*. Oxford: Academic Press, pp. 102–112. https://doi.org/10.1016/B978-0-444-52512-3.00233-3

Balzarolo, M., Valdameri, N., Fu, Y.H., Schepers, L., Janssens, I.A. & Campioli, M. (2019) Different determinants of radiation use efficiency in cold and temperate forests. *Global Ecology and Biogeography*, 28, 1649–1667. Available from: https://doi.org/10.1111/geb.12985

Behmann, J., Acebron, K., Emin, D., Bennertz, S., Matsubara, S. & Thomas, S. et al. (2018) Specim IQ: evaluation of a new, miniaturized handheld hyperspectral camera and its application for plant phenotyping and disease detection. *Sensors (Switzerland)*, 18(2), 441. Available from: https://doi.org/10.3390/s18020441

Blumenthal, D.M., Mueller, K.E., Kray, J.A., LeCain, D.R., Pendall, E., Duke, S. et al. (2018) Warming and elevated CO_2 interact to alter seasonality and reduce variability of soil water in a semiarid grassland. *Ecosystems*, 21, 1533–1544. Available from: https://doi.org/10.1007/s10021-018-0237-1

Bonan, G.B., Patton, E.G., Finnigan, J.J., Baldocchi, D.D. & Harman, I.N. (2021) Moving beyond the incorrect but useful paradigm: reevaluating big-leaf and multilayer plant canopies to model biosphere-atmosphere fluxes—a review. *Agricultural and Forest Meteorology*, 306, 108435. Available from: https://doi.org/10.1016/j.agrformet.2021.108435

Bonfil, D.J. (2017) Wheat phenomics in the field by RapidScan: NDVI vs. NDRE. *Israel Journal of Plant Science*, 64, 41–54. Available from: https://doi.org/10.1080/07929978.2016.1249135

Busch, F.A. (2013) Current methods for estimating the rate of photorespiration in leaves. *Plant Biology*, 15, 648–655. Available from: https://doi.org/10.1111/j.1438-8677.2012.00694.x

Busch, F.A. (2020) Photorespiration in the context of Rubisco biochemistry, CO_2 diffusion and metabolism. *The Plant Journal*, 101, 919–939. Available from: https://doi.org/10.1111/tpj.14674

Von Caemmerer, S. (2000) *Biochemical models of leaf photosynthesis*. Collingwood: CSIRO Publishing, 165 pp.

Chaudhary, N., Bonfil, D.J. & Tas, E. (2021) Physiological and yield responses of spring wheat cultivars under realistic and acute levels of ozone. *Atmosphere*, 12, 1392. Available from: https://doi.org/10.3390/atmos12111392

Christy, B., Tausz-Posch, S., Tausz, M., Richards, R., Rebetzke, G., Condon, A. et al. (2018) Benefits of increasing transpiration efficiency in wheat under elevated CO_2 for rainfed regions. *Global Change Biology*, 24, 1965–1977. Available from: https://doi.org/10.1111/gcb.14052

Cohen, Y., Alchanatis, V., Sela, E., Saranga, Y., Cohen, S., Meron, M. et al. (2015) Crop water status estimation using thermography: multi-year model development using ground-based thermal images. *Precision Agriculture*, 16, 311–329. Available from: https://doi.org/10.1007/s11119-014-9378-1

Cornic, G. (2000) Drought stress inhibits photosynthesis by decreasing stomatal aperture—not by affecting ATP synthesis. *Trends in Plant Science*, 5, 187–188. Available from: https://doi.org/10.1016/S1360-1385(00)01625-3

Demmig-Adams, B. & Adams, W.W. (2006) Photoprotection in an ecological context: the remarkable complexity of thermal energy dissipation. *New Phytologist*, 172, 11–21. Available from: https://doi.org/10.1111/j.1469-8137.2006.01835.x

Deryng, D., Elliott, J., Folberth, C., Müller, C., Pugh, T.A.M., Boote, K.J. et al. (2016) Regional disparities in the beneficial effects of rising CO_2 concentrations on crop water productivity. *Nature Climate Change*, 6, 786–790. Available from: https://doi.org/10.1038/nclimate2995

Dusenge, M.E., Duarte, A.G. & Way, D.A. (2019) Plant carbon metabolism and climate change: elevated CO_2 and temperature impacts on photosynthesis, photorespiration and respiration. *New Phytologist*, 221, 32–49. Available from: https://doi.org/10.1111/nph.15283

Eisenhut, M., Bräutigam, A., Timm, S., Florian, A., Tohge, T., Fernie, A.R. et al. (2017) Photorespiration is crucial for dynamic response of photosynthetic metabolism and stomatal movement to altered CO_2 availability. *Molecular Plant*, 10, 47–61. Available from: https://doi.org/10.1016/j.molp.2016.09.011

Eller, F., Hyldgaard, B., Driever, S.M. & Ottosen, C.O. (2020) Inherent trait differences explain wheat cultivar responses to climate factor interactions: new insights for more robust crop modelling. *Global Change Biology*, 26, 5965–5978. Available from: https://doi.org/10.1111/gcb.15278

Evain, S. (2004) A new instrument for passive remote sensing: 2. Measurement of leaf and canopy reflectance changes at 531 nm and their relationship with photosynthesis and chlorophyll fluorescence. *Remote Sensing of Environment*, 91, 175–185. Available from: https://doi.org/10.1016/j.rse.2004.03.012

Ewert, F., Rodriguez, D., Jamieson, P., Semenov, M.A., Mitchell, R.A.C., Goudriaan, J. et al. (2002) Effects of elevated CO_2 and drought on wheat: testing crop simulation models for different experimental and climatic conditions. *Agriculture, Ecosystems & Environment*, 93, 249–266. Available from: https://doi.org/10.1016/S0167-8809(01)00352-8

Filella, I. (2004) Reflectance assessment of seasonal and annual changes in biomass and CO_2 uptake of a Mediterranean shrubland submitted to experimental warming and drought. *Remote Sensing of Environment*, 90, 308–318. Available from: https://doi.org/10.1016/j.rse.2004.01.010

Fréchette, E., Wong, C.Y.S., Junker, L.V., Chang, C.Y.Y. & Ensminger, I. (2015) Zeaxanthin-independent energy quenching and alternative electron sinks cause a decoupling of the relationship between the photochemical reflectance index (PRI) and photosynthesis in an evergreen conifer during spring. *Journal of Experimental Botany*, 66, 7309–7323. Available from: https://doi.org/10.1093/jxb/erv427

Fuchs, M. & Tanner, C.B. (1966) Infrared thermometry of vegetation 1. *Agronomy Journal*, 58, 597–601. Available from: https://doi.org/10.2134/agronj1966.00021962005800060014x

Gamon, J.A., Kitajima, K., Mulkey, S.S., Serrano, L. & Wright, S.J. (2005) Diverse optical and photosynthetic properties in a neotropical dry forest during the dry season: implications for remote estimation of photosynthesis. *Biotropica*, 37, 547–560. Available from: https://doi.org/10.1111/j.1744-7429.2005.00072.x

Gamon, J.A., Peñuelas, J. & Field, C.B. (1992) A narrow-waveband spectral index that tracks diurnal changes in photosynthetic efficiency. *Remote Sensing of Environment*, 41, 35–44. Available from: https://doi.org/10.1016/0034-4257(92)90059-S

Gamon, J.A., Serrano, L. & Surfus, J.S. (1997) The photochemical reflectance index: an optical indicator of photosynthetic radiation use efficiency across species, functional types, and nutrient levels. *Oecologia*, 112, 492–501. Available from: https://doi.org/10.1007/s004420050337

Gamon, J.A., Somers, B., Malenovský, Z., Middleton, E.M., Rascher, U. & Schaepman, M.E. (2019) Assessing vegetation function with imaging spectroscopy. *Surveys in Geophysics*, 40, 489–513. Available from: https://doi.org/10.1007/s10712-019-09511-5

Gara, T.W., Skidmore, A.K., Darvishzadeh, R. & Wang, T. (2019) Leaf to canopy upscaling approach affects the estimation of canopy traits. *GIScience & Remote Sensing*, 56, 554–575. Available from: https://doi.org/10.1080/15481603.2018.1540170

Garbulsky, M.F., Peñuelas, J., Gamon, J., Inoue, Y. & Filella, I. (2011) The photochemical reflectance index (PRI) and the remote sensing of leaf, canopy and ecosystem radiation use efficiencies. A review and meta-analysis. *Remote Sensing of Environment*, 115, 281–297. Available from: https://doi.org/10.1016/j.rse.2010.08.023

Garrity, S.R., Eitel, J.U.H. & Vierling, L.A. (2011) Disentangling the relationships between plant pigments and the photochemical reflectance index reveals a new approach for remote estimation of carotenoid content. *Remote Sensing of Environment*, 115, 628–635. Available from: https://doi.org/10.1016/j.rse.2010.10.007

Gates, D.M. (1968) Transpiration and leaf temperature. *Annual Review of Plant Physiology*, 19, 211–238. Available from: https://doi.org/10.1146/annurev.pp.19.060168.001235

Gitz III, D.C., Baker, J.T. & Lascano, R.J. (2016) Scaling leaf measurements to estimate whole canopy gas exchanges of cotton. *American Journal of Plant Sciences*, 07, 1952–1963. Available from: https://doi.org/10.4236/ajps.2016.714178

Gray, S.B., Dermody, O., Klein, S.P., Locke, A.M., McGrath, J.M. & Paul, R.E. et al. (2016) Intensifying drought eliminates the expected benefits of elevated carbon dioxide for soybean. *Nature Plants*, 2, 16132. Available from: https://doi.org/10.1038/nplants.2016.132

Helman, D., Bonfil, D.J. & Lensky, I.M. (2019) Crop RS-Met: a biophysical evapotranspiration and root-zone soil water content model for crops based on proximal sensing and meteorological data. *Agricultural Water Management*, 211, 210–219. Available from: https://doi.org/10.1016/j.agwat.2018.09.043

Helman, D., Lensky, I.M. & Bonfil, D.J. (2019) Early prediction of wheat grain yield production from root-zone soil water content at heading using crop RS-Met. *Field Crops Research*, 232, 11–23. Available from: https://doi.org/10.1016/j.fcr.2018.12.003

Helman, D., Lensky, I.M., Osem, Y., Rohatyn, S., Rotenberg, E. & Yakir, D. (2017) A biophysical approach using water deficit factor for daily estimations of evapotranspiration and CO_2 uptake in Mediterranean environments. *Biogeosciences*, 14, 3909–3926. Available from: https://doi.org/10.5194/bg-14-3909-2017

Helman, D., Yungstein, Y., Mulero, G. & Michael, Y. (2022). High-Throughput Remote Sensing of Vertical Green Living Walls (VGWs) in Workplaces. *Remote Sensing*, 14(14), 3485. https://doi.org/10.3390/rs14143485

Herrmann, I. & Berger, K. (2021) Remote and proximal assessment of plant traits. *Remote Sensing*, 13, 1893. Available from: https://doi.org/10.3390/rs13101893

Hilker, T., Lyapustin, A., Hall, F.G., Wang, Y., Coops, N.C., Drolet, G. et al. (2009) An assessment of photosynthetic light use efficiency from space: modeling the atmospheric and directional impacts on PRI reflectance. *Remote Sensing of Environment*, 113, 2463–2475. Available from: https://doi.org/10.1016/j.rse.2009.07.012

Hmimina, G., Dufrêne, E. & Soudani, K. (2014) Relationship between photochemical reflectance index and leaf ecophysiological and biochemical parameters under two different water statuses: towards a rapid and efficient correction method using real-time measurements. *Plant, Cell & Environment*, 37, 473–487. Available from: https://doi.org/10.1111/pce.12171

Huang, Q., Qiu, F., Fan, W., Liu, Y. & Zhang, Q. (2019) Evaluation of different methods for estimating the fraction of sunlit leaves and its contribution for photochemical reflectance index utilization in a coniferous forest. *Remote Sensing*, 11(4), 1643. Available from: https://doi.org/10.3390/rs11141643

Inoue, Y. (1991) Remote and real-time sensing of transpiration and stomatal resistance based on infrared thermometry. *Japan Agricultural Research Quarterly*, 25, 159–164.

Jarvis, P.G. (1995) Scaling processes and problems. *Plant, Cell and Environment*, 18, 1079–1089. Available from: https://doi.org/10.1111/j.1365-3040.1995.tb00620.x

Jiang, D., Mulero, G., Bonfil, D.J. & Helman, D. (2022) Early or late? The role of genotype phenology in determining wheat response to drought under future high atmospheric CO_2 levels. *Plant, Cell & Environment*, 45(12), 3445–3461. Available from: https://doi.org/10.1111/pce.14430

Jones, H.G., Serraj, R., Loveys, B.R., Xiong, L., Wheaton, A. & Price, A.H. (2009) Thermal infrared imaging of crop canopies for the remote diagnosis and quantification of plant responses to water stress in the field. *Functional Plant Biology*, 36, 978–989. Available from: https://doi.org/10.1071/FP09123

Jones, P., Allen, L.H., Jones, J.W., Boote, K.J. & Campbell, W.J. (1984) Soybean canopy growth, photosynthesis, and transpiration responses to whole-season carbon dioxide enrichment 1. *Agronomy Journal*, 76, 633–637. Available from: https://doi.org/10.2134/agronj1984.00021962007600040030x

Kangasjarvi, S., Neukermans, J., Li, S., Aro, E.M. & Noctor, G. (2012) Photosynthesis, photorespiration, and light signalling in defence responses. *Journal of Experimental Botany*, 63, 1619–1636. Available from: https://doi.org/10.1093/jxb/err402

Katul, G.G., Oren, R., Manzoni, S., Higgins, C. & Parlange, M.B. (2012) Evapotranspiration: a process driving mass transport and energy exchange in the soil–plant–atmosphere–climate system. *Reviews of Geophysics*, 50, 1–25. Available from: https://doi.org/10.1029/2011RG000366

Kim, Y., Still, C.J., Roberts, D.A. & Goulden, M.L. (2018) Thermal infrared imaging of conifer leaf temperatures: comparison to thermocouple measurements and assessment of environmental influences. *Agricultural and Forest Meteorology*, 248, 361–371. Available from: https://doi.org/10.1016/j.agrformet.2017.10.010

Kimball, B.A. (2016) Crop responses to elevated CO_2 and interactions with H_2O, N, and temperature. *Current Opinion in Plant Biology*, 31, 36–43. Available from: https://doi.org/10.1016/j.pbi.2016.03.006

Klein, T., Cohen, S. & Yakir, D. (2011) Hydraulic adjustments underlying drought resistance of *Pinus halepensis*. *Tree Physiology*, 31, 637–648. Available from: https://doi.org/10.1093/treephys/tpr047

Klein, T., Shpringer, I., Fikler, B., Elbaz, G., Cohen, S. & Yakir, D. (2013) Relationships between stomatal regulation, water-use, and water-use efficiency of two coexisting key Mediterranean tree species. *Forest Ecology and Management*, 302, 34–42. Available from: https://doi.org/10.1016/j.foreco.2013.03.044

Kohzuma, K., Tamaki, M. & Hikosaka, K. (2021) Corrected photochemical reflectance index (PRI) is an effective tool for detecting environmental stresses in agricultural crops under light conditions. *Journal of Plant Research*, 134, 683–694. Available from: https://doi.org/10.1007/s10265-021-01316-1

Kováč, D., Veselovská, P., Klem, K., Večeřová, K., Ač, A. & Peñuelas, J. et al. (2018) Potential of photochemical reflectance index for indicating photochemistry and light use efficiency in leaves of European beech and Norway spruce trees. *Remote Sensing*, 10(8), 1202. Available from: https://doi.org/10.3390/rs10081202

Lapidot, O., Ignat, T., Rud, R., Rog, I., Alchanatis, V. & Klein, T. (2019) Use of thermal imaging to detect evaporative cooling in coniferous and broadleaved tree species of the Mediterranean maquis. *Agricultural and Forest Meteorology*, 271, 285–294. Available from: https://doi.org/10.1016/j.agrformet.2019.02.014

Leakey, A.D.B., Ainsworth, E.A., Bernacchi, C.J., Rogers, A., Long, S.P. & Ort, D.R. (2009) Elevated CO_2 effects on plant carbon, nitrogen, and water relations: six important lessons from FACE. *Journal of Experimental Botany*, 60, 2859–2876. Available from: https://doi.org/10.1093/jxb/erp096

Lima, R.S.N., García-Tejero, I., Lopes, T.S., Costa, J.M., Vaz, M., Durán-Zuazo, V.H. et al. (2016) Linking thermal imaging to physiological indicators in *Carica papaya* L. under different watering regimes. *Agricultural Water Management*, 164, 148–157. Available from: https://doi.org/10.1016/j.agwat.2015.07.017

Liu, B.B., Li, M., Li, Q.M., Cui, Q.Q., Zhang, W.D., Ai, X.Z. et al. (2018) Combined effects of elevated CO_2 concentration and drought stress on photosynthetic performance and leaf structure of cucumber (*Cucumis sativus* L.) seedlings. *Photosynthetica*, 56, 942–952. Available from: https://doi.org/10.1007/s11099-017-0753-9

Long, S.P., Ainsworth, E.A., Rogers, A. & Ort, D.R. (2004) Rising atmospheric carbon dioxide: plants FACE the future. *Annual Review of Plant Biology*, 55, 591–628. Available from: https://doi.org/10.1146/annurev.arplant.55.031903.141610

Magney, T.S., Vierling, L.A., Eitel, J.U.H., Huggins, D.R. & Garrity, S.R. (2016) Response of high frequency photochemical reflectance index (PRI) measurements to environmental conditions in wheat. *Remote Sensing of Environment*, 173, 84–97. Available from: https://doi.org/10.1016/j.rse.2015.11.013

Manfreda, S., McCabe, M.F., Miller, P.E., Lucas, R., Madrigal, V.P. & Mallinis, G. et al. (2018) On the use of unmanned aerial systems for environmental monitoring. *Remote Sensing*, 10(4), 641. Available from: https://doi.org/10.3390/rs10040641

Matese, A., Baraldi, R., Berton, A., Cesaraccio, C., Di Gennaro, S., Duce, P. et al. (2018) Estimation of water stress in grapevines using proximal and remote sensing methods. *Remote Sensing*, 10, 114. Available from: https://doi.org/10.3390/rs10010114

Miller, O., Helman, D., Svoray, T., Morin, E. & Bonfil, D.J. (2019) Explicit wheat production model adjusted for semi-arid environments. *Field Crops Research*, 231, 93–104. Available from: https://doi.org/10.1016/j.fcr.2018.11.011

Moller, M., Alchanatis, V., Cohen, Y., Meron, M., Tsipris, J., Naor, A. et al. (2006) Use of thermal and visible imagery for estimating crop water status of irrigated grapevine. *Journal of Experimental Botany*, 58, 827–838. Available from: https://doi.org/10.1093/jxb/erl115

Monteith, J.L. (1977) Climate and the efficiency of crop production in Britian. *Philosophical Transactions of the Royal Society B: Biological Sciences*, 281, 277–294.

Muller, J.D., Rotenberg, E., Tatarinov, F., Oz, I. & Yakir, D. (2021a) Evidence for efficient nonevaporative leaf-to-air heat dissipation in a pine forest under drought conditions. *New Phytologist*, 232, 2254–2266. Available from: https://doi.org/10.1111/nph.17742

Muller, J.D., Rotenberg, E., Tatarinov, F., Vishnevetsky, I., Dingjan, T., Kribus, A. et al. (2021b) 'Dual-reference' method for high-precision infrared measurement of leaf surface temperature under field conditions. *New Phytologist*, 232, 2535–2546. Available from: https://doi.org/10.1111/nph.17720

Niinemets, Ü., Keenan, T.F. & Hallik, L. (2015) A worldwide analysis of within-canopy variations in leaf structural, chemical and physiological traits across plant functional types. *New Phytologist*, 205, 973–993. Available from: https://doi.org/10.1111/nph.13096

O'Leary, G.J., Christy, B., Nuttall, J., Huth, N., Cammarano, D., Stöckle, C. et al. (2015) Response of wheat growth, grain yield and water use to elevated CO_2 under a free-air CO_2 enrichment (FACE) experiment and modelling in a semi-arid environment. *Global Biological Change*, 21, 2670–2686. Available from: https://doi.org/10.1111/gcb.12830

Paudel, I., Halpern, M., Wagner, Y., Raveh, E., Yermiyahu, U., Hoch, G. et al. (2018) Elevated CO_2 compensates for drought effects in lemon saplings via stomatal downregulation, increased soil moisture, and increased wood carbon storage. *Environmental and Experimental Botany*, 148, 117–127. Available from: https://doi.org/10.1016/j.envexpbot.2018.01.004

Peñuelas, J., Filella, I. & Gamon, J.A. (1995) Assessment of photosynthetic radiation-use efficiency with spectral reflectance. *New Phytologist*, 131, 291–296. Available from: https://doi.org/10.1111/j.1469-8137.1995.tb03064.x

Peñuelas, J., Garbulsky, M.F. & Filella, I. (2011) Photochemical reflectance index (PRI) and remote sensing of plant CO_2 uptake. *New Phytologist*, 191, 596–599. Available from: https://doi.org/10.1111/j.1469-8137.2011.03791.x

Porcar-Castell, A., Garcia-Plazaola, J.I., Nichol, C.J., Kolari, P., Olascoaga, B., Kuusinen, N. et al. (2012) Physiology of the seasonal relationship between the photochemical reflectance index and photosynthetic light use efficiency. *Oecologia*, 170, 313–323. Available from: https://doi.org/10.1007/s00442-012-2317-9

Rogers, A., Dietz, K.-J., Gifford, M.L. & Lunn, J.E. (2021) The importance of independent replication of treatments in plant science. *Journal of Experimental Botany*, 72, 5270–5274. Available from: https://doi.org/10.1093/jxb/erab268

Rogers, A., Medlyn, B.E., Dukes, J.S., Bonan, G., Caemmerer, S., Dietze, M.C. et al. (2017) A roadmap for improving the representation of photosynthesis in Earth system models. *New Phytologist*, 213, 22–42. Available from: https://doi.org/10.1111/nph.14283

Sagan, V., Maimaitijiang, M., Sidike, P., Eblimit, K., Peterson, K.T. & Hartling, S. et al. (2019) UAV-based high resolution thermal imaging for vegetation monitoring, and plant phenotyping using ICI 8640 P, FLIR Vue Pro R 640, and thermomap cameras. *Remote Sensing*, 11(3), 330. Available from: https://doi.org/10.3390/rs11030330

Shiff, S., Lensky, I.M. & Bonfil, D.J. (2021) Using satellite data to optimize wheat yield and quality under climate change. *Remote Sensing*, 13(11), 2049. Available from: https://doi.org/10.3390/rs13112049

Smigaj, M., Gaulton, R., Suarez, J.C. & Barr, S.L. (2017) Use of miniature thermal cameras for detection of physiological stress in conifers. *Remote Sensing*, 13(11), 957. Available from: https://doi.org/10.3390/rs9090957

Still, C., Powell, R., Aubrecht, D., Kim, Y., Helliker, B. & Roberts, D. et al. (2019) Thermal imaging in plant and ecosystem ecology: applications and challenges. *Ecosphere*, 10(6), e02768. Available from: https://doi.org/10.1002/ecs2.2768

Still, C.J., Rastogi, B., Page, G.F.M., Griffith, D.M., Sibley, A., Schulze, M. et al. (2021) Imaging canopy temperature: shedding (thermal) light on ecosystem processes. *New Phytologist*, 230, 1746–1753. Available from https://doi.org/10.1111/nph.17321

Sukhov, V., Sukhova, E., Khlopkov, A., Yudina, L., Ryabkova, A. & Telnykh, A. et al. (2021) Proximal imaging of changes in photochemical reflectance index in leaves based on using pulses of green–yellow light. *Remote Sensing*, 13, 1762.

Swann, A.L.S., Hoffman, F.M., Koven, C.D. & Randerson, J.T. (2016) Plant responses to increasing CO_2 reduce estimates of climate impacts on drought severity. *Proceedings of the National Academy of Sciences of*

the United States of America, 113, 10019–10024. Available from: https://doi.org/10.1073/pnas.1604581113

Takahashi, S. & Badger, M.R. (2011) Photoprotection in plants: a new light on photosystem II damage. *Trends in Plant Science*, 16, 53–60. Available from: https://doi.org/10.1016/j.tplants.2010.10.001

Tausz-Posch, S., Norton, R.M., Seneweera, S., Fitzgerald, G.J. & Tausz, M. (2013) Will intra-specific differences in transpiration efficiency in wheat be maintained in a high CO_2 world? A FACE study. *Physiologia Plantarum*, 148, 232–245. Available from: https://doi.org/10.1111/j.1399-3054.2012.01701.x

Tausz-Posch, S., Tausz, M. & Bourgault, M. (2020) Elevated [CO_2] effects on crops: advances in understanding acclimation, nitrogen dynamics and interactions with drought and other organisms. *Plant Biology*, 22, 38–51. Available from: https://doi.org/10.1111/plb.12994

Thenkabail, P.S., Lyon, J.G. & Huete, A. (2016) *Hyperspectral remote sensing of vegetation*. Boca Raton, FL, USA: CRC Press.

Tubiello, F.N. & Ewert, F. (2002) Simulating the effects of elevated CO_2 on crops: approaches and applications for climate change. *European Journal of Agronomy*, 18, 57–74. Available from: https://doi.org/10.1016/S1161-0301(02)00097-7

Uprety, D.C., Garg, S.C., Bisht, B.S., Maini, H.K., Dwivedi, N., Paswan, G. et al. (2006) Carbon dioxide enrichment technologies for crop response studies. *Journal of Scientific and Industrial Research (India)*, 65, 859–866.

Urban, J., Ingwers, M., McGuire, M.A. & Teskey, R.O. (2017) Stomatal conductance increases with rising temperature. *Plant Signaling & Behavior*, 12(8), e1356534. Available from: https://doi.org/10.1080/15592324.2017.1356534

Vialet-Chabrand, S. & Lawson, T. (2019) Dynamic leaf energy balance: deriving stomatal conductance from thermal imaging in a dynamic environment. *Journal of Experimental Botany*, 70, 2839–2855. Available from: https://doi.org/10.1093/jxb/erz068

Voss, I., Sunil, B., Scheibe, R. & Raghavendra, A.S. (2013) Emerging concept for the role of photorespiration as an important part of abiotic stress response. *Plant Biology*, 15, 713–722. Available from: https://doi.org/10.1111/j.1438-8677.2012.00710.x

Wada, S., Suzuki, Y. & Miyake, C. (2020) Photorespiration enhances acidification of the thylakoid lumen, reduces the plastoquinone pool, and contributes to the oxidation of P700 at a lower partial pressure of CO_2 in wheat leaves. *Plants*, 9, 319. Available from: https://doi.org/10.3390/plants9030319

Wall, G.W., Garcia, R.L., Kimball, B.A., Hunsaker, D.J., Pinter Jr., P.J., Long, S.P. et al. (2006) Interactive effects of elevated carbon dioxide and drought on wheat. *Agronomy Journal*, 98, 354–381. Available from: https://doi.org/10.2134/agronj2004.0089

Wu, C., Huang, W., Yang, Q. & Xie, Q. (2015) Improved estimation of light use efficiency by removal of canopy structural effect from the photochemical reflectance index (PRI). *Agriculture, Ecosystems & Environment*, 199, 333–338. Available from: https://doi.org/10.1016/j.agee.2014.10.017

Wullschleger, S.D., Gunderson, C.A., Hanson, P.J., Wilson, K.B. & Norby, R.J. (2002) Sensitivity of stomatal and canopy conductance to elevated CO_2 concentration—interacting variables and perspectives of scale. *New Phytologist*, 153, 485–496. Available from: https://doi.org/10.1046/j.0028-646X.2001.00333.x

Wullschleger, S.D. & Norby, R.J. (2001) Sap velocity and canopy transpiration in a sweetgum stand exposed to free-air CO_2 enrichment (FACE). *New Phytologist*, 150, 489–498. Available from: https://doi.org/10.1046/j.1469-8137.2001.00094.x

Zhang, C., Filella, I., Garbulsky, M.F. & Peñuelas, J. (2016) Affecting factors and recent improvements of the photochemical reflectance index (PRI) for remotely sensing foliar, canopy and ecosystemic radiation-use efficiencies. *Remote Sensing*, 8(9), 677. Available from:https://doi.org/10.3390/rs8090677

Zhang, C., Filella, I., Liu, D., Ogaya, R., Llusià, J., Asensio, D. et al. (2017) Photochemical reflectance index (PRI) for detecting responses of diurnal and seasonal photosynthetic activity to experimental drought and warming in a Mediterranean shrubland. *Remote Sensing*, 9, 1189. Available from: https://doi.org/10.3390/rs9111189

Zhang, Y.J., Hou, M.Y., Xue, H.Y., Liu, L.T., Sun, H.C., Li, C.D. et al. (2018) Photochemical reflectance index and solar-induced fluorescence for assessing cotton photosynthesis under water-deficit stress. *Biologia Plantarum*, 62, 817–825. Available from: https://doi.org/10.1007/s10535-018-0821-4

SUPPORTING INFORMATION

Additional supporting information can be found online in the Supporting Information section at the end of this article.

How to cite this article: Mulero, G., Jiang, D., Bonfil, D. J. & Helman, D. (2023) Use of thermal imaging and the photochemical reflectance index (PRI) to detect wheat response to elevated CO_2 and drought. *Plant, Cell & Environment*, 46, 76–92. https://doi.org/10.1111/pce.14472